Journal of Hydraulic Research Vol. 43, No. 5 (2005), pp. 540–548

Experimental study of transition and skimming flows on stepped spillways in RCC dams: qualitative analysis and pressure measurements

Etude expérimentale des écoulements de transition et de déversement sur des déversoirs en escalier des barrages en béton compacté (RCC): analyses qualitatives et mesures de pression

M. SÁNCHEZ-JUNY, *Hydraulic, Maritime and Environmental Engineering Department, UPC, Street Jordi Girona 1-3, Edifici D-1, 08034 Barcelona, Spain. E-mail: marti.sanchez@upc.edu*

J. DOLZ, *Hydraulic, Maritime and Environmental Engineering Department, UPC, Street Jordi Girona 1-3, Edifici D-1, 08034 Barcelona, Spain*

ABSTRACT
This paper is a presentation of an experimental facility used for analyzing the flow over the stepped spillway of an RCC dam. The technique of digitizing video sequences is applied in order to obtain a qualitative analysis of the hydraulic behavior of these chutes. The onset of skimming flow is studied using two different criteria: a visual criterion and another that makes use of the pressure pattern on the horizontal faces of the steps. The evolution along the length of the spillway of pressures measured on the centers of symmetry of the horizontal faces of the steps is also analyzed to obtain further conclusions regarding hydraulic behavior during a skimming flow regime.

RÉSUMÉ
Cet article présente un équipement expérimental utilisé pour analyser l'écoulement sur le déversoir en escalier d'un barrage RCC. On a utilisé la technique de numérisation des séquences vidéo pour obtenir une analyse qualitative du comportement hydraulique de ces chutes. Le début de l'écoulement de déversement est étudié en utilisant deux différents critères: un critère visuel et un autre qui utilise le champ de pression sur les faces horizontales des étages. L'évolution, sur la longueur du déversoir, des pressions mesurées au centre de symétrie des faces horizontales des étages est également analysée pour obtenir des conclusions supplémentaires sur le comportement hydraulique pendant un régime d'écoulement de déversement.

Keywords: Stepped spillway, RCC dam, skimming flow, transition flow, pressure evolution.

1 Introduction and objectives

Design discharges used in stepped spillways in RCC dams develop over the chute a particular regime (skimming flow). Therefore the different flow patterns over these spillways will be discussed. Particularly the flow behavior during the onset of skimming flow will be examined, attending the changes in pressure evolution from high to low discharges. But, the main scope of this paper is analyzing this flow pattern observed for design discharges by means of introducing the technique of digitizing video sequences and showing the evolution along the spillway of pressures on the center of the step tread.

2 Experimental facilities

The experimental data presented in this paper were obtained from experimentation on a stepped chute, 4.30 m high (from crest to toe), with a slope of 1v:0.8 h and a width of 0.6 m. It consisted of 40 identical steps 0.10 m high (h), plus five steps at the top of the model fitted to a Creager profile (Sánchez-Juny, 2001). The model was built of transparent methacrylate, in order to allow the flow to be visual inspected. The maximum discharge tested was 200 l/s, i.e., $y_c/h = 2.25$, y_c being the critical depth.

To be able to locate any point above a step of the spillway the variables showed in Fig. 1 were defined.

3 Flow categories on the stepped spillway of an RCC dam

As is well described in all the classic references on the hydraulics of stepped spillways (Chanson, 2002), hydraulic behavior can be characterized as belonging to one of three different types, depending on the discharge: nappe, transition and skimming flow. Furthermore, the geometric characteristics of a stepped spillway over an RCC dam (chute slope around 1v:0.8h and step height around 0.9–1.2 m) are responsible for some of the specific aspects of this hydraulic behavior.

Revision received October 21, 2004/Open for discussion until August 31, 2006.

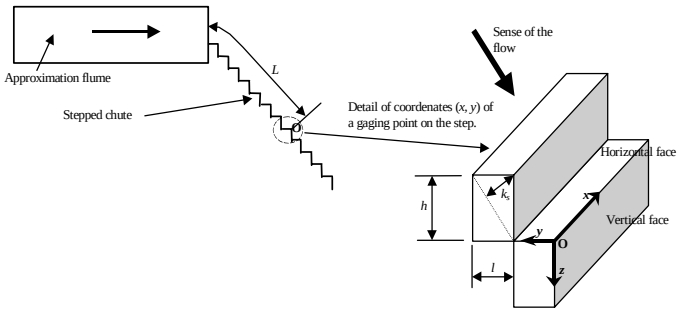

Figure 1 Notation utilized to locate any point on the steps analyzed (after Sánchez-Juny *et al.*, 2000).

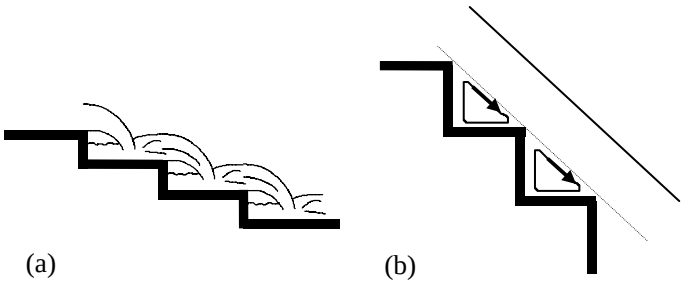

Figure 2 Nappe flow (a) and skimming flow (b) over a stepped spillway.

3.1 Nappe flow

Nappe flow was observed for low discharges. It is characterized by water forming a pulsing plate as it falls from one step to the next one down. The presence of a cell filled with air—between the upper flow, the vertical face of the step and the small plunge formed over the horizontal face of the step—is the main characteristic of this regime, as is shown in Fig. 2(a). Due to the short length of the horizontal face of the steps in RCC stepped spillways—not more than 1 m—the formation of a clean-cut hydraulic jump on each step is avoided. The observations on the physical model built in the Laboratory show this nappe flow for discharges under the limits $y_c/h = 0.57$ and $y_c/h = 0.67$.

As discharges increase, the cells of air described above are alternately filled with a mesh of water and air showing a steady rotation. The flow regime on a stepped spillway depends on the discharge and the step geometry (Chanson, 2002; Boes and Hager, 2003; Ohtsu *et al.*, 2004).

3.2 Transition flow

3.2.1 Visual description

From nappe flow, and for increasing discharges, the recent works (Pinheiro and Fael, 2000; Amador *et al.*, 2002; Chanson, 2002;) agree that a transition flow is developed, until the onset of skimming flow was considered to have occurred when the air-filled cells trapped beneath the upper main flow and the vertical face of the step filled with an air–water mesh along the entire length of the spillway (Chanson, 1994), as can be seen in Fig. 3. The same criterion had already been used by other authors (Pinheiro and Fael, 2000). On the other hand, Chamani and Rajaratnam (1999) established that incipient skimming flow in stepped spillways shows that the jet becomes parallel to the slope of the chute. The last criterion fits quite well with the experimental results obtained only in stepped spillways with high slopes, i.e., $h/l > 1$.

The transition flow observed over the tested experimental spillway ($h/l = 1.25$) was established for discharges greater than those which limit nappe flow, and lower than a value of y_c/h between 0.77 and 0.83.

These values coincide with the estimated threshold of the onset of skimming flow that had been established by Rajaratnam (1990) by using the expression $y_c/h = 0.80$, which had in turn been obtained from experimental data from Essery and Horner (1978).

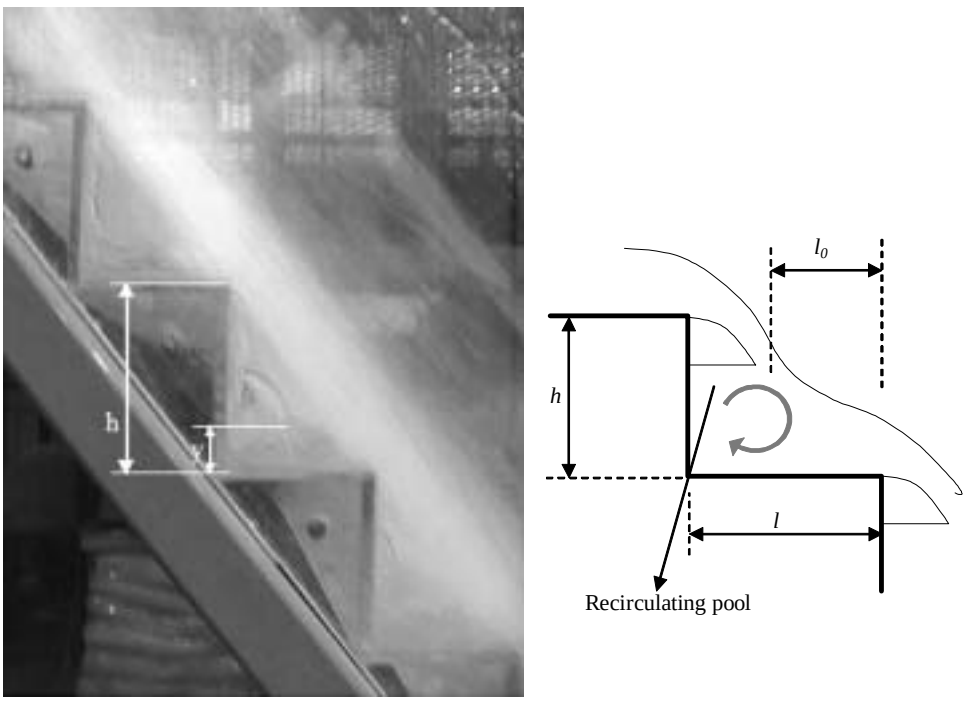

Figure 3 A visual description of the onset of skimming flow is established by $y \approx h$.

Chanson (1994), using this experimental data, developed an equation to determine the onset of skimming flow based on the channel slope.

3.2.2 Pressure description

Time series of pressure along the tread of the step at which $L/ks = 69.66$ (the 11th step from the downstream end) are plotted in Figs 4 and 5. Skimming flow occurred the beginning of the test ($t = 0$ s) and at the end ($t = 30$ s) nappe flow was achieved, as is shown in Fig. 3. During the skimming flow regime the pressures on the tread of the step appear to be dependent upon their position on the step, which means that the highest and most variable pressures are those that were recorded closest to the external edge. Furthermore, in a skimming flow regime two different regions can be pointed out on the tread of the step, as was already described in Sánchez-Juny (2001). They are:

— The downstream half of the horizontal face. Along this surface, pressure tends to increase and reaches maximum values at the outer edges. This zone is characterized by the impact of the upper flow.

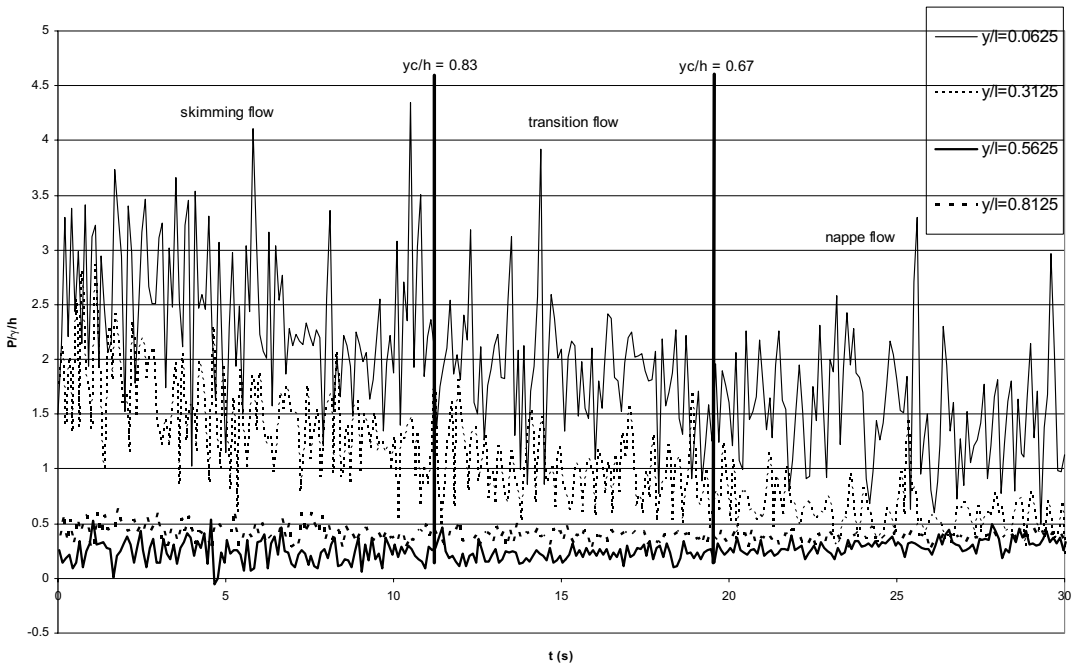

Figure 4 Time series of dimensionless pressure recorded along the tread of the step at which $L/k_s = 69.66$ (the 11th step from the downstream end). The dimensionless positions, y/l, of the recording points are described in Fig. 1.

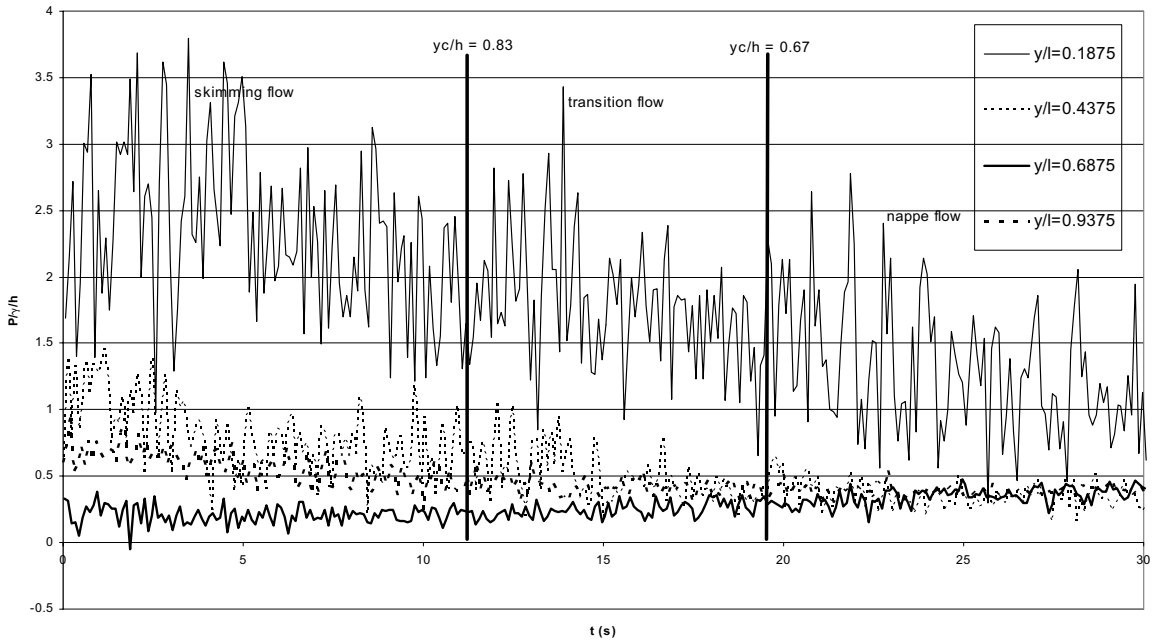

Figure 5 Time series of dimensionless pressure recorded along the tread of the step at which $L/k_s = 69.66$ (the 11th step from the downstream end). The dimensionless positions, y/l, of the recording points are described in Fig. 1.

— The upstream half of the horizontal face. This is characterized by a boundary separation of the flow. Therefore, the larger the discharge is down the chute, the lower pressures and fluctuations are obtained in this region.

At the end of the test a clear nappe flow occurred. In this case it can again be observed that the tread of the step can be divided into two zones, which are slightly different from the ones described for skimming flow. They are:

— The downstream quarter of the horizontal face. Again, pressure tends to increase the closer a point is to the outer edges. This zone is also characterized by the impact of the upper flow. The maximum pressures in the outer end of the steps show values around three times the step height (Amador *et al.*, 2002).
— The upstream three quarters of the horizontal face, which are characterized by a hydrostatic behavior. Therefore, in this region the different measuring points tend to show the same pressure according to the water level, as was pointed out in Fig. 3. In this case the lower the discharge is, the lower the pressure fluctuations are (Amador *et al.*, 2001).

Between initial skimming flow and the final nappe flow, a transition regime is observed. In this transition flow pressures on the upstream region, which are initially governed by the eddy trapped under the skimming flow, begin to show the hydrostatic pattern.

3.3 Skimming flow

For even greater discharges the cells trapped along the entire length of the chute become filled by the rotating air–water mesh, as can be seen in Fig. 2(b). This is typically referred to as skimming flow.

The conditions of the flow must be modified in order for there to occur an interference such that will cause the entrance of air. This is dependent upon the properties of the fluid and typically occurs when inertia forces overcome viscosity and surface tension forces. In general, a minimum speed must be overcome, as air entrainment is induced by turbulent fluctuations in the flow. Thus, the critical point will be defined (Wood *et al.*, 1983) as the point of air entrainment in the flow. In great slope channels, this point is the point where the boundary layer reaches the flow surface.

Inertia in the flow over the chute is most likely the cause of its inability to follow the edges of the stepped geometry. Therefore, a boundary separation of the flow is observed once the transition to a skimming flow is complete. This moment is characterized by the formation of an eddy with a horizontal axis between two contiguous external edges. It occurs in such a manner that the flow is supported not only by the external edges of the steps, but by the internal eddies as well. Therefore a virtual surface forms that leans on those edges, and over which the main flow passes (Fig. 2(b)). This virtual surface acts as a pseudo-bottom for the upper main flow.

For typical slopes of spillways in RCC dams ($h/l \approx 1.25$), recirculatory flow occupies the whole cavity limited by the external edges of two contiguous steps. Stable recirculations were observed for cavities with a relation h/l between 0.40 and 0.45 (Chanson, 1994). If the spillway height is long enough, quasi-uniform conditions can be achieved (Ohtsu *et al.*, 2004).

In the following Sections 4 and 5, a more accurate description of skimming flow regime will be carried out. Particularly, in Section 4 a qualitative analysis using digitized video sequences is showed and in Section 5 the pressures along the center of the horizontal faces of the steps are analyzed and they are related to the behavior of the pseudo-bottom.

4 Qualitative analysis of the skimming flow

4.1 Focuses of this analysis

The test facilities consisted of a domestic video recorder, which allowed a recording to be made of the flow over the spillway in several locations and for several different discharges. Once the various sequences were recorded, they were digitized through an A/D interface.

The digitizing process consisted in transforming each point in every frame into an integer value representative of the light intensity recorded there. Thus, the intensity scale goes from 0 (black) to 255 (white), which is why it is called the *grayscale*. The digitized sequences were processed using DIGIMAGE. This package was developed by the Mathematics and Theoretical Physics Department of Cambridge University. The software processes the image as a set of points (pixels) over a 512×512-pixel grid. In order to better appreciate the different values associated with the light intensity, the software allows for the use of different scales with false colors, so that a color is assigned to each value of the light intensity and a fictitious image is created which allows those pixels with the greatest light intensity to be easily highlighted. In Fig. 6 a digitized frame using a false color scale is shown.

This software allows rows or columns to be fixed within a sequence and the light intensity time series to be analyzed along

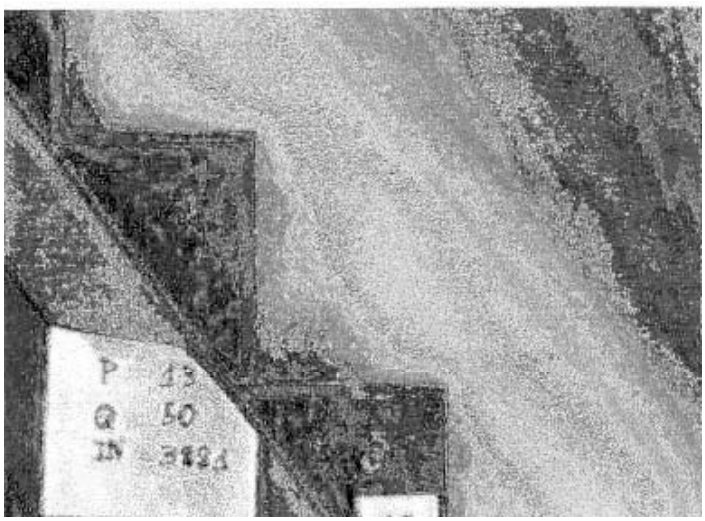

Figure 6 View of a digitized image, using a false color scale. The darker the color is the lower the light intensity is, and vice versa.

them. In Fig. 7 an example of the light intensity time series along a column is shown over 20 s. Therefore, the possibility of studying time series along certain preset rows and columns allows one to examine a grid defined *a priori*. Figure 8 shows the grid that was examined.

While the evolution of the mean light intensity only shows some qualitative information about the mean flow, further and more interesting information is given by the variance. Likewise, the variation over time of the light intensity is due to the same flow variability. This, in other words, is the intensity of the turbulence at that point. Therefore, the estimation of the variability of light intensity (variance) should at least be a qualitative estimator of the intensity of the turbulence. Therefore, one of the objectives of this paper was to obtain, although in a qualitative way, maps of the variation of variance (or standard deviation) of light intensity time series for each point of the defined grid.

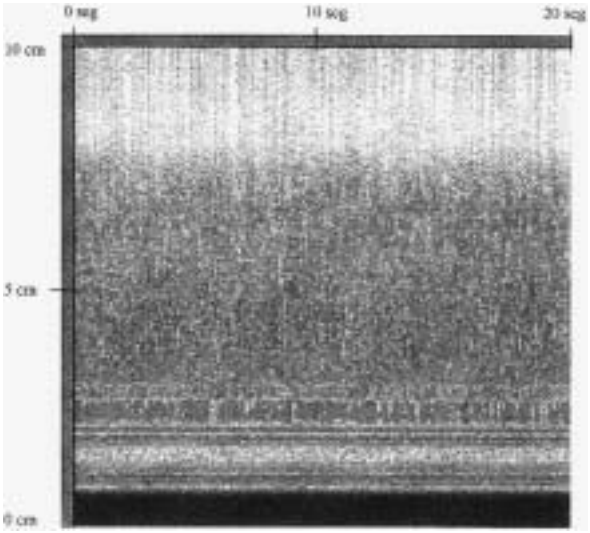

Figure 7 Example of the evolution of light intensity in 20 s' time along a vertical.

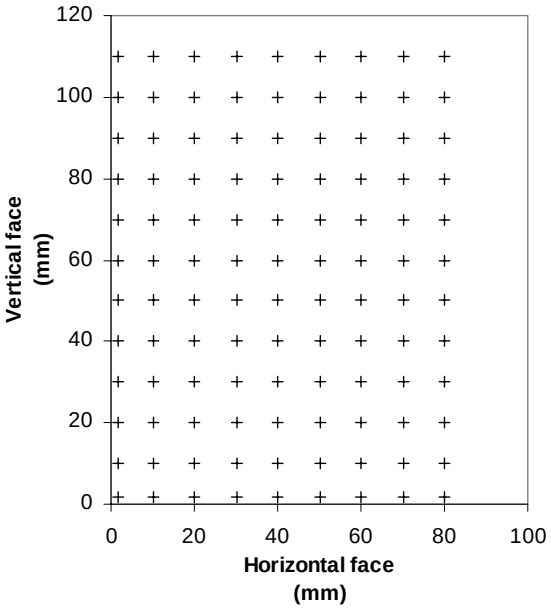

Figure 8 Image of the working grid for the study region.

4.2 Results

Given the experimental data, it can be deduced that in a cell under the skimming flow the area where the largest fluctuation in the flow occurs should be at the friction surface between the trapped vortex and the upper skimming flow. Figure 9 gives a qualitative account of the intensity of this fluctuation, which was obtained by digitizing a video sequence. These intensity fluctuations are estimated by the variability of light intensity time series, on the pixels of the screen. This parameter is somewhat complex due to its dependence on the lighting system (Quintilla, 1999). Figure 9 also shows the different patterns obtained by means of natural lighting (A) and frontal lighting using a 500 W lamp (B). Two different characteristics of the flow are evidenced by both maps—namely, that:

— Natural lighting emphasizes the friction surface.
— Frontal lighting with a 500 W lamp shows more clearly the fluctuation intensity inside the cell under the skimming flow.

An analysis of the correlation matrix allows for the estimation of the integral scales of that flow. Figure 10 shows the results obtained using frontal lighting emanating from a 500 W lamp.

— The integral time scale is defined as:

$$L_t = \int_0^{+\infty} R_t(\tau)\,\mathrm{d}\tau. \tag{1}$$

Here, R_t is the correlation coefficient between two time series, on the same pixel, with a time shift, τ.

— In the same way the integral length scale can be defined as:

$$L_e = \int_0^{+\infty} R_e(\chi)\,\mathrm{d}\chi. \tag{2}$$

where R_e is the correlation coefficient between time series in two different points, x and $x + \chi$, with the same time origin. Therefore, the integral length scale could be conceived of as a measurement of the large eddies in the turbulent flow.

In Map A (Fig. 10) a maximum length scale value of around 6 cm can be observed, as in this case the analysis was done going in the horizontal direction. These values correspond to points located near the pseudo-bottom, which approximately correspond to the thickness of the flow over the steps. Inside the cell, values range from 4 cm near the upper skimming flow to 1 cm near the boundary. Therefore, the characteristics of the flow at a point near the center of the cell are influenced by flow conditions that are further away than those that would affect it if the point were near a step face.

Map B (Fig. 10) shows that, in the main flow zone over the trapped eddy, the values of the integral time scale range between 30 and 50 ms. These are, approximately, the lowest time scales that can be determined with the recording equipment used in this experiment. The authors believe that the values in this zone should be slightly lower, but the equipment was unable to detect them. In Map B, the results seem to suggest that the nearer a point

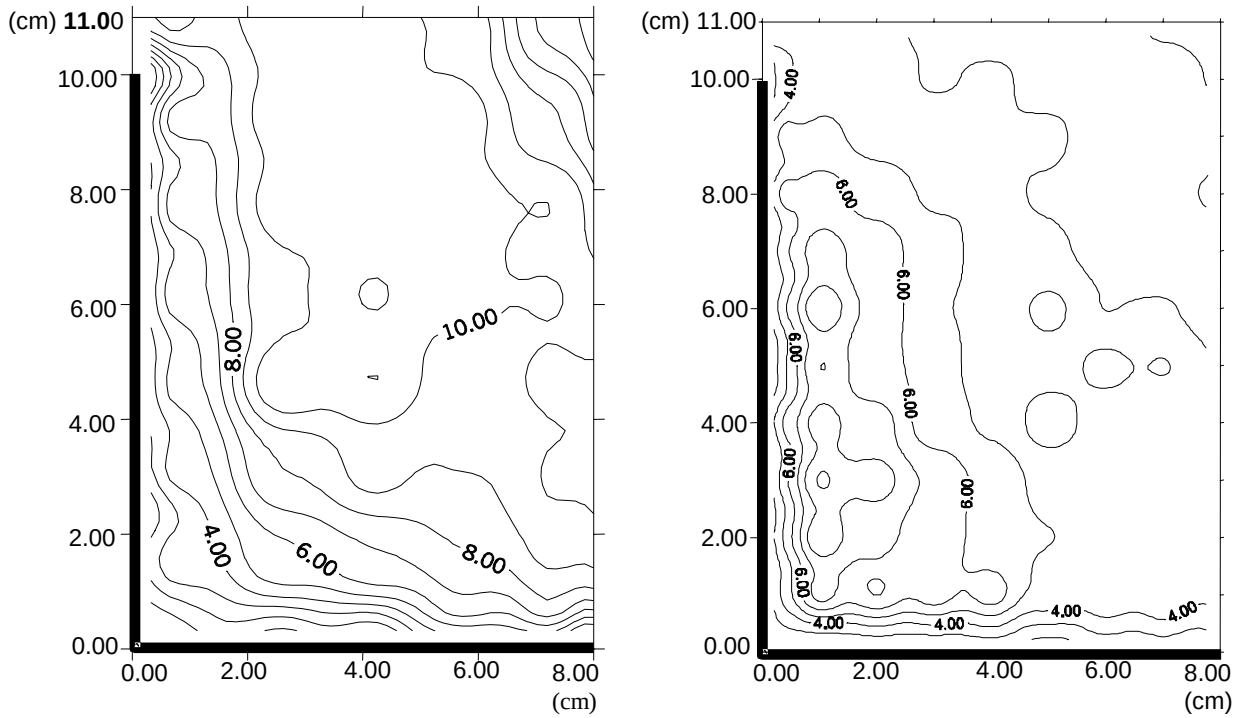

Figure 9 Comparison of maps of equal standard deviation of light intensity, for natural lighting (A)—after Sánchez-Juny *et al.* (1996, 1998)—and frontal lighting with a 500 W lamp (B)—after Quintilla (1999). ($L/k_s = 69.663$).

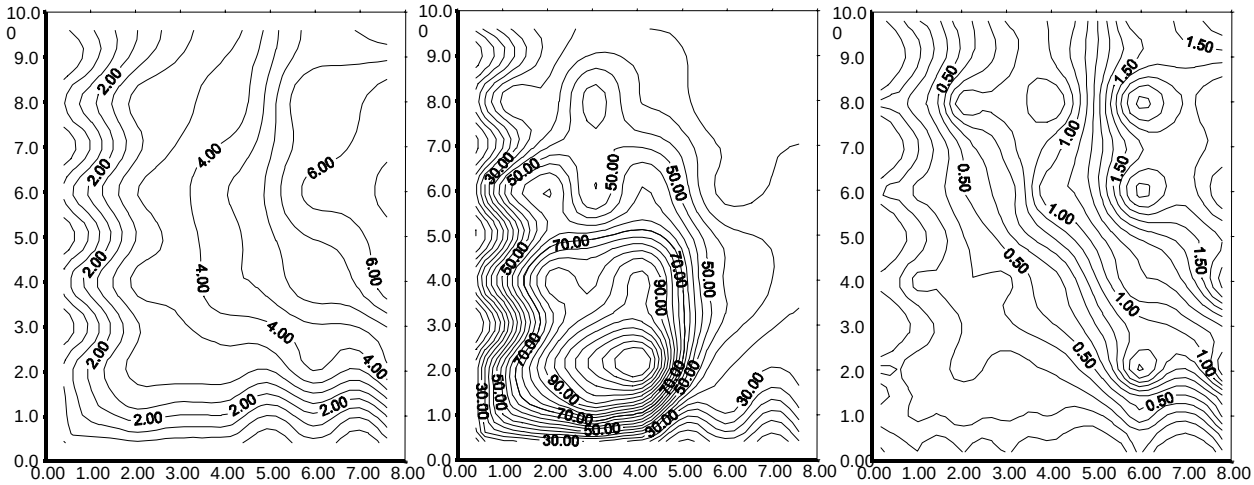

Figure 10 Integral length scale (A), integral time scale (B) and characteristic velocity (C) inside a cell, estimated by means of digitized flow video sequences, with frontal lighting using a 500 W lamp ($L/k_s = 69.663$ and $y_c/h = 0.891$).

is to the center of the cell, the longer the flow characteristics will be influenced by the flow behavior mentioned above.

Map C (Fig. 10) is obtained by dividing the values in Map A by those estimated in Map B. In this graph there is a steep velocity gradient around the virtual surface between the upper skimming flow and the lower cell. It is important to point out that values for characteristic velocities in the graph may be susceptible to error because of the degree of accuracy of the system. Furthermore, it can be appreciated that the vortex inside the lower cell is not as well defined as might be expected. The authors believe that more work should be done on the lighting conditions of the flow.

5 Pressures along the center of the horizontal faces of the steps

5.1 Description

The graphs in Figs 11–14 show the pressure evolution for discharges ranging from $y_c/h = 0.891$ to $y_c/h = 2.25$ along the

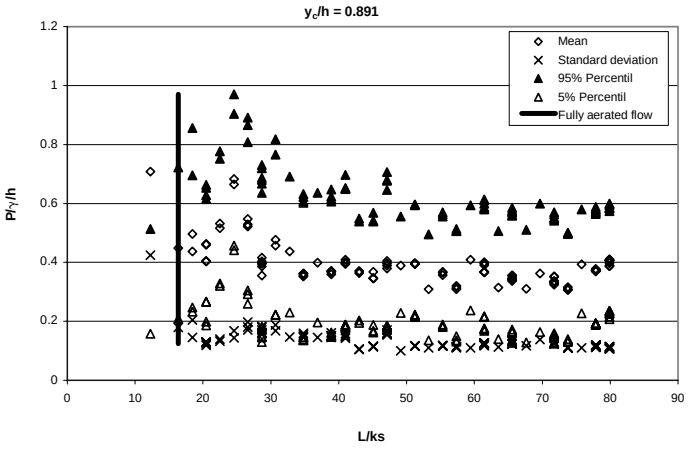

Figure 11 Pressure evolution along a stepped chute obtained for $y_c/h = 0891$. Points of measurement were located on the center of symmetry of the horizontal faces of the steps.

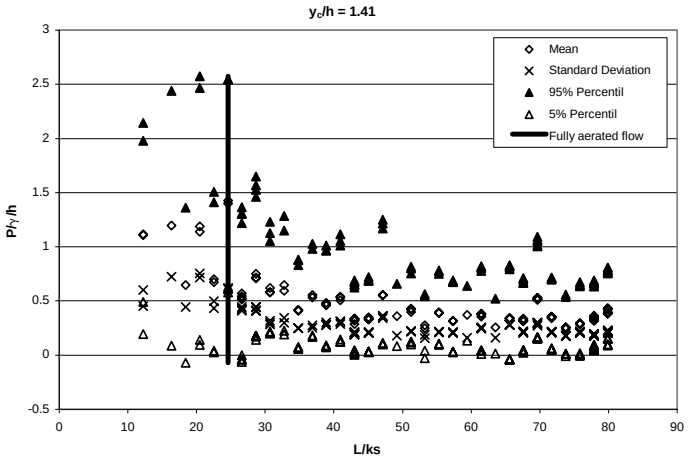

Figure 12 Pressure evolution along a stepped chute obtained for $y_c/h = 1.41$. Points of measurement were located on the center of symmetry of the horizontal faces of the steps.

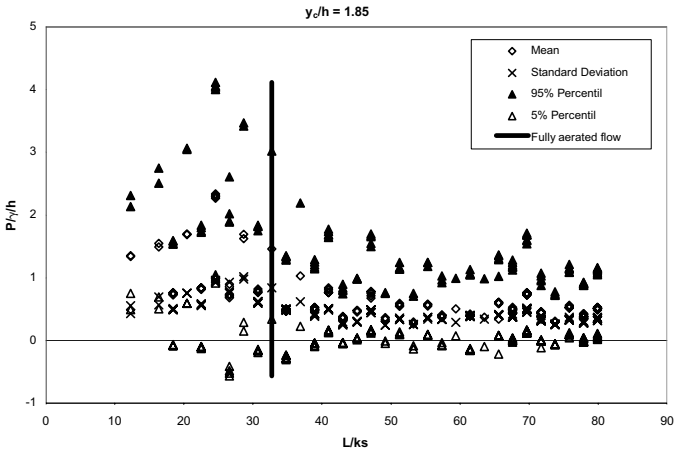

Figure 13 Pressure evolution along a stepped chute obtained for $y_c/h = 1.85$. Points of measurement were located on the center of symmetry of the horizontal faces of the steps.

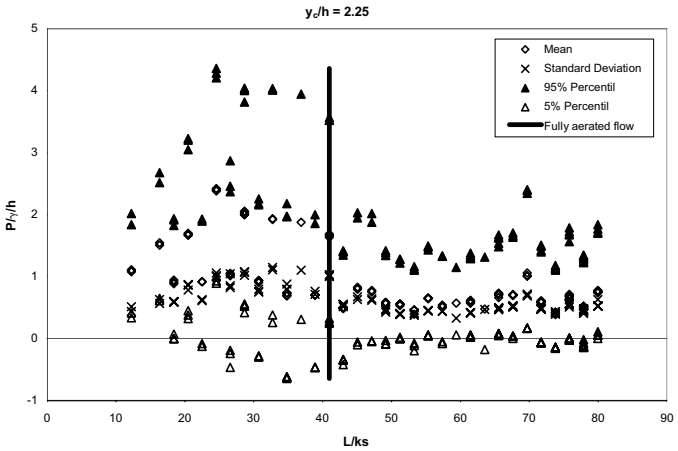

Figure 14 Pressure evolution along a stepped chute obtained for $y_c/h = 2.25$. Points of measurement were located on the center of symmetry of the horizontal faces of the steps.

center of symmetry of the horizontal faces of the steps. The discharges tested ensured a skimming flow. Those graphs also show a plot of the points where the flow could be considered to have been fully aerated. The statistical variables used are: mean, standard deviation and 95th and 5th percentiles. The measurements at each point were repeated at least twice, and at certain points as many as five times. All the measurements carried out are shown in order to justify the repeatability of the phenomenon.

— Upstream of the inception point of the boundary layer (where the air entrainment is initiated), the pressures undergo a greater variability than downstream, where the flow is fully developed. The same tendencies are shown in CEMAGREF (1991).
— The mean pressures are positive all along the spillway. Only minimum pressures exhibit negative values, although these values are far from indicating a risk of cavitation, at least at the center of symmetry of the horizontal face.
— The maximum and minimum pressures are located upstream of the point of inception of the boundary layer.
— The pressures that were measured exhibited a steady wavy pattern down the chute. Similar behavior was already presented by Othsu and Yasuda (1997), in a stepped spillway for a skimming flow regime with a 19° slope.

5.2 Discussion

The behavior of the mean pressure and the standard deviation along the zone of fully developed flow, have been enlarged in the graphs shown in Fig. 15. These graphs show the approximately steady wavy behavior, mentioned above, which can even be seen to have a phase coincidence (coincidence of maximum and minimum when taking into account different discharges).

It can be seen that the greater the discharge, the higher the mean pressures were, though the lowest mean pressures obtained were always greater than $p/\gamma h = 0.25$. At no point do negative mean pressures occur, due to the significant aeration of the flow in this area. The steady wavy behavior is not so clearly evident for the lowest flow tested ($y_c/h = 0.891$), which appears to be

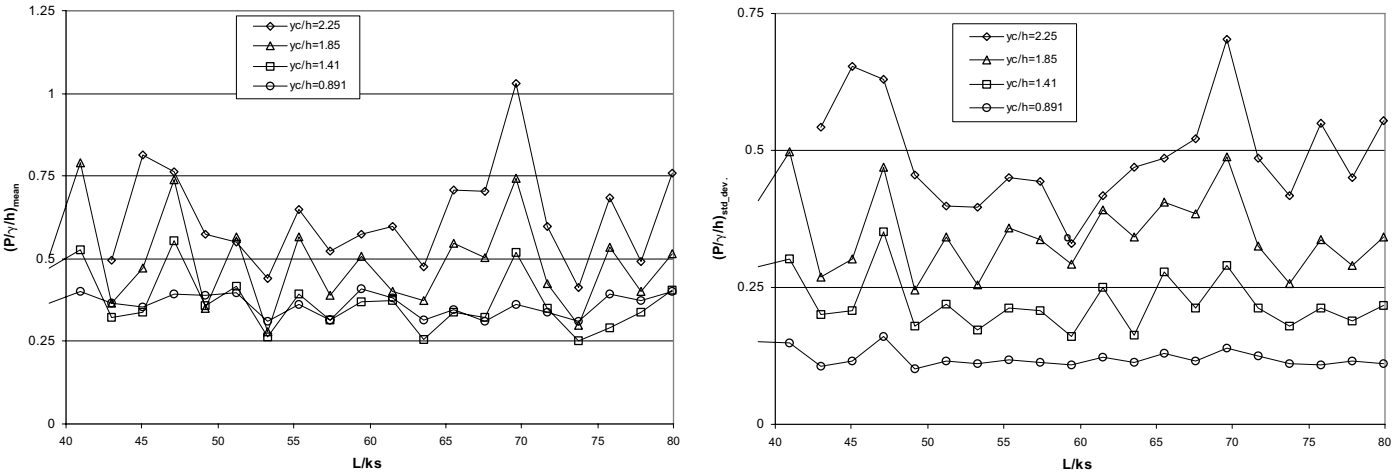

Figure 15 Mean pressure (left) and standard deviation (right) evolution over the center of symmetry of the horizontal face of the steps, in the zone of fully–developed skimming flow.

close to the onset of the skimming flow regime, as is shown in Section 3.2.2. This seems to be logical, since in the nappe flow regime an identical hydraulic behavior occurs on all the steps.

A steady wavy pattern is shown in the evolution of the standard deviation along the center of symmetry of the spillway steps. Here, the various evolutions exhibit a much better segregation by discharge, so that the bigger the discharge the higher the resulting variability of pressures is. The standard deviation obtained for the lowest discharge ($y_c/h = 0.891$), shows an important cushioning of the steady wavy behavior if one compares it with the evolutions obtained at higher discharges.

This wavy pattern of the pressures along the center of symmetry of the tread of the steps, seems to indicate that, although a stable recirculation exists the main eddies are not always in the same position. Therefore, the pseudo-bottom between the upper main flow and the secondary flow in the cavities is not exactly defined by the external edges of the steps, but it can hit or separate of them.

6 Conclusions

Some tests were developed using a hydraulic model of a stepped spillway operated under Froude similitude criteria. These tests were dedicated to simulate the hydraulic behavior of these structures, which point out the following conclusions:

— That the onset of skimming flow regime can be analyzed according to two different criteria:
  - First, by using a *visual description*: when the cells filled with air trapped beneath the upper main flow and the vertical face of the step become filled by the air–water mesh along the entire length of the spillway. Using this criterion $y_c/h = 0.80$ for $h/l = 1.25$ is obtained.
  - And second, by using a *pressure description*: in other words, when the pressure on the upstream three quarters of the horizontal face of the step exhibits hydrostatic behavior.

— Though digitized video sequences provide a non-intrusive useful technique for performing a qualitative analysis of the flow, more work should be carried out in order to determine the influence of the lighting process on the results.

— The pressure along the center of symmetry of the horizontal faces of steps for skimming flow shows a wavy pattern. This wavy pattern points out the different position of eddies trapped in the cavities under the pseudo-bottom along the spillway.

Notation

y_c = critical depth in a rectangular section
h = length of the vertical face of the step
l = length of the horizontal face of the step
L = distance from the crest of the spillway to the external edge of step
k_s = roughness height of a step measured perpendicular to the flow direction
O = Origin of the coordinates located on each step at the extreme right (following the direction of the flow) of the external edge of the step
x = coordinate defined over the edge of the step from right to left. It varies from 0 to the channel width
y = coordinate which defines the distance over the horizontal face of the step to the external edge of the step. It ranges from 0 to l
z = coordinate which defines the distance over the vertical face of the step to the external edge of the step. It ranges from 0 to h
t = time
L_t = turbulence integral time scale
L_e = turbulence integral length scale
R_t = correlation coefficient between two time series, on a same pixel, with a time shift τ
R_e = correlation coefficient between two time series, in two different points, x and $x + \xi$, with the same time origin

τ = time shift
p = pressure
γ = specific weight of water

References

1. AMADOR, A., VALENZANO, B., SÁNCHEZ-JUNY, M., POMARES, J. and DOLZ, J. (2002). "Estudio del campo de presiones en el paso de flujo escalón a escalón a flujo rasante". *Proc. of XX Lantinoamerican Congress of Hydralics. IAHR*. La Habana. Cuba.
2. BOES, R. and HAGER, W.H. (2003). "Hydraulic Design of Stepped Spillways". *J. Hydraul. Eng., ASCE* 129(9), 671–679.
3. CEMAGREF (1991). "Étude de la dissipation d'energie sur les evacuateurs a marches". Projet National BaCaRa. Raport d'essais Société du Canal de Provence et d'Aménagement de la Région Provençale. 116 pp.
4. CHAMANI, M. and RAJARATNAM, N. (1999). "Onset of Skimming Flow on Stepped Spillways". *J. Hydraul. Eng., ASCE* 125(9), 969–971.
5. CHANSON, H. (1994). *Hydraulic Design of Stepped Cascades, Channels, Weirs and Spillways*. Pergamon, 260 pp.
6. CHANSON, H. (2002). *The Hydraulics of Stepped Chutes and Spillways*. Balkema, 384 pp.
7. ESSERY, I.T.S. and HORNER, M.N. (1978). The Hydraulic Design of Stepped Spillways. Ciria Report 33. London, 45 pp.
8. OHTSU, I., YASUDA, Y. and TAKAHASHI, M. (2004). "Flow Characteristics of Skimming Flow in Stepped Channels". *J. Hydraul. Eng., ASCE* 130(9), 860–869.
9. PINHEIRO, A. and FAEL, C. (2000). "Nappe Flow in Stepped Channels. Occurrence and Energy Dissipation". *Proceedings of the International Workshop of Hydraulics of Stepped Spillways*. Balkema, Zurich, pp. 119–126.
10. QUINTILLA, R. (1999). "Caracterización del flujo rasante sobre un aliviadero escalonado en presas de HCC. Aplicación de la técnica de digitalización de imágenes". Undergraduate research work directed by M. Sánchez-Juny. School of Civil Engineering of Barcelona (ETSECCPB), UPC. Barcelona, 108 pp.
11. RAJARATNAM, N. (1990). "Skimming Flow in Stepped Spillways". *J. Hydraul. Eng., ASCE* 116(4), 587–591.
12. SÁNCHEZ-JUNY, M. and DOLZ, J. (1996). "Aliviaderos escalonados: acciones mecánicas". III Course of Roller Compacted Concrete Dams. IECA. Madrid, pp. 59–74. Published in the IECA Reference (1999).
13. SÁNCHEZ-JUNY, M., POMARES, J., NINYEROLA, D., POLO, J. and DOLZ, J. (1998). "Caracterización del campo de presiones sobre un aliviadero escalonado". *Proceedings of the XVIII Congress of the IAHR Latin American Division*. Oaxaca, México, pp. 609–618.
14. SÁNCHEZ-JUNY, M., POMARES, J. and DOLZ, J. (2000). "Pressure Field in Skimming Flor Over a Stepped Spillway". *Proceedings of the International Workshop of Hydraulics of Stepped Spillways*. Balkema, Zurich, pp. 137–145.
15. SÁNCHEZ-JUNY, M. (2001). "Comportamiento hidráulico de los aliviaderos escalonados en presas de hormigón compactado. Análisis del campo de presiones". PhD Thesis, Technical University of Catalonia (UPC). Directed by Dr. J. Dolz. Barcelona. 328 pp.
16. WOOD, I.R., ACKERS, P. and LOVELESS, J. (1983). "General Method for Critical Point on Spillways". *J. Hydraul. Eng., ASCE* 109(2), 308–312.